Available online at www.sciencedirect.com
SCIENCE DIRECT®
Precambrian Research 133 (2004) 329–337
Precambrian Research
www.elsevier.com/locate/precamres

SHRIMP U–Pb dating of diagenetic xenotime in the Stirling Range Formation, Western Australia: 1.8 billion year minimum age for the Stirling biota

Birger Rasmussen [a,*], Ian R. Fletcher [a], Stefan Bengtson [b], Neal J. McNaughton [a]

[a] *School of Earth and Geographical Sciences, University of Western Australia, Crawley, WA 6009, Australia*
[b] *Department of Palaeozoology, Swedish Museum of Natural History, Box 50007, SE-104 05 Stockholm, Sweden*

Received 18 November 2003; accepted 27 May 2004

Abstract

The Stirling Range Formation in southwestern Australia contains discoidal fossils previously linked to the late Neoproterozoic Ediacaran biota and possible trace fossils interpreted to have been made by vermiform, mucus-producing, motile organisms. The age of the sedimentary succession was recently reported to be between 2.0 and 1.2 billion years old, based on U–Pb geochronology of detrital zircon and metamorphic monazite, respectively. Ion microprobe U–Pb geochronology of xenotime in sandstones from the same succession produces three sets of radiometric data. Detrital xenotime grains yield ages between 3120 and 2100 Ma (consistent with the detrital zircon data; between 3460 and 1960 Ma), whereas compositionally distinct xenotime overgrowths yield a weighted mean $^{207}Pb/^{206}Pb$ age of 1800 ± 14 Ma for the oldest population and 1662 ± 15 Ma for a younger population. The new data show that the Stirling Range Formation is more than 1.8 billion years old, some 600 million years older than the minimum defined by metamorphic monazite. The results show that the various megascopic fossils reported in the succession are between 2.0 and 1.8 billion years old, emphasizing their already controversial nature. If our interpretation of the fossils is correct, then motile multicellular (or possibly syncytial) organisms had already emerged in the late Paleoproterozoic, simultaneously with the first large alga-like multicellular eukaryotes.

Keywords: Stirling biota; Xenotime; SHRIMP; Geochronology; Multicellular life; Trace fossils

1. Introduction

In the early 1990s, discoidal impressions with presumed affinities to the Ediacaran biota were discovered in the Stirling Range Formation in southwestern Australia (Cruse, 1991; Cruse et al., 1993; Cruse and Harris, 1994) (Fig. 1). At the time, the only available age data were a limited number of Rb–Sr analyses that indicated that the succession had a metamorphic age of approximately 1124 Ma (Turek and Stephenson, 1966). However, with the discovery of fossils resembling Ediacaran forms, a latest Neoproterozoic age was inferred, and the Rb–Sr dates were subsequently considered to reflect the ages of detrital grains (Harris, 1994).

Recent U–Pb age dating of the Stirling Range Formation indicates that the succession is between 2.0 and 1.2 billion years old (Rasmussen et al., 2002a).

* Corresponding author. Tel.: +61-8-6488-1871; fax: +61-8-6488-1037.
E-mail address: brasmuss@segs.uwa.edu.au (B. Rasmussen).

0301-9268/$ – see front matter © 2004 Elsevier B.V. All rights reserved.
doi:10.1016/j.precamres.2004.05.008

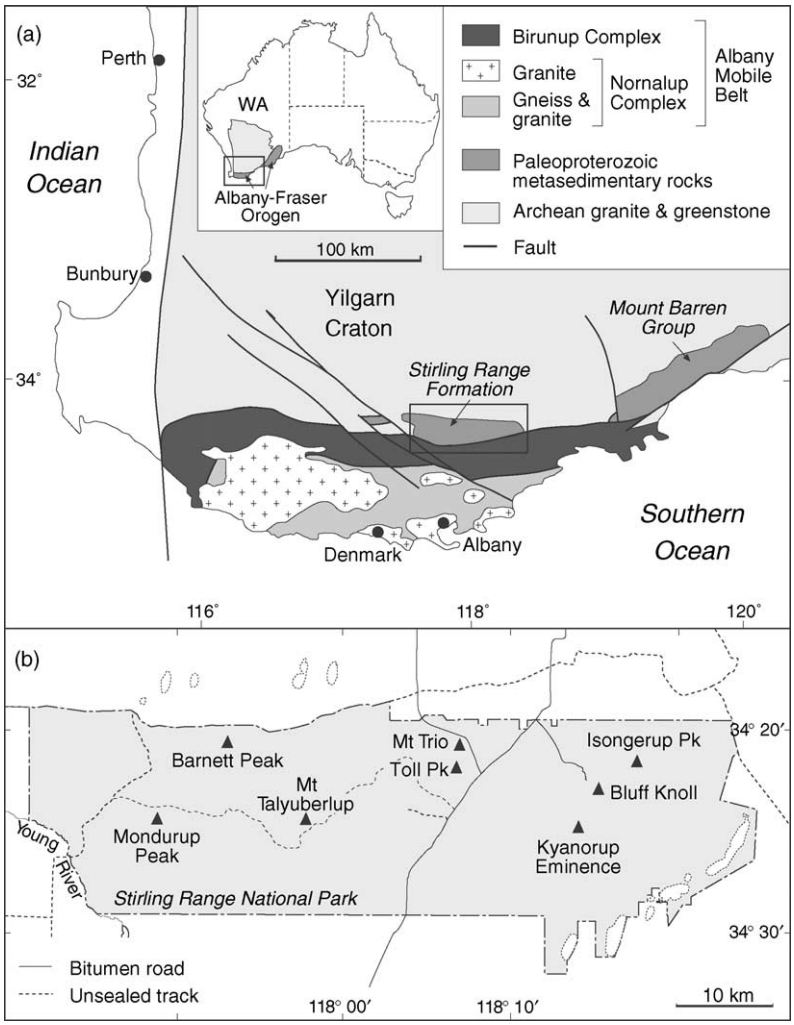

Fig. 1. (a) Simplified geological map of the Stirling Range Formation and Albany–Fraser Orogen in southwestern Australia. (b) Map showing the location of geochronology sample sites (black triangles) within the Stirling Range National Park.

The age bracket was determined by radiometric dating of detrital zircon and metamorphic monazite for the upper and lower age, respectively. From these same rocks Rasmussen et al. (2002a) reported trace-like fossils interpreted to have been made by vermiform, mucus-producing organisms, an interpretation questioned by Conway Morris (2002) and Budd and Jensen (2003). More precise dating of the Stirling Range Formation will clearly be crucial to assess the nature and significance of these controversial fossils, and we have now obtained radiometric dates from diagenetic xenotime (YPO_4), restricting the age of the Stirling Range Formation to between 2.0 and 1.8 Ga.

2. Geological setting and sample details

The Stirling Range Formation is an approximately 1.6 km thick succession of quartzite, shale, slate and phyllite, located in southwestern Australia along the southern margin of the Archean Yilgarn Craton and the northern boundary of the Mesoproterozoic Albany–Fraser Orogen (Fig. 1a) (Muhling and

Brakel, 1985). The sedimentary rocks have undergone sub-greenschist to lower greenschist facies metamorphism and several episodes of deformation (Boulter, 1979; Muhling and Brakel, 1985; Beeson, 1991). Based on an Ediacaran age, the deformational events recorded in the Stirling Range Formation were interpreted to reflect Lower Paleozoic compression related to Gondwanaland assembly (Harris and Beeson, 1993). However, recent sensitive high-resolution ion microprobe (SHRIMP) U–Pb dating of monazite indicates that the succession was metamorphosed approximately 1200 Ma (Rasmussen et al., 2002a) during the Albany–Fraser orogeny between approximately 1300 Ma and 1140 Ma (Black et al., 1992; Clark et al., 1999; 2000).

The Stirling Range Formation is intruded by a series of east–west trending dolerite dykes thought to be Upper Cambrian to Lower Ordovician in age from paleomagnetic dating (Harris and Beeson, 1993; Harris and Li, 1995). However, SHRIMP U–Pb analysis of zirconolite in five of the dykes indicates that they were emplaced at 1218 ± 3 Ma (Rasmussen and Fletcher, in press) and subsequently deformed during compressional reactivation of intracontinental structures after 1190 Ma. Dyke emplacement is contemporaneous with, and the probable cause of, peak thermal metamorphism in the orogen (Dawson et al., 2003; Rasmussen and Fletcher, in press), an event that is responsible for the growth of metamorphic monazite (1215 ± 20 Ma) in the Stirling Range Formation (Rasmussen et al., 2002a).

To constrain the age of the Stirling Range Formation further, samples of sandstone were collected from the Barnett Peak section that contains the disputed fossils, as well as from seven other localities (Fig. 1b). Polished thin sections (PTS; 56 in total) were examined by scanning electron microscope (SEM; JEOL 6400) for the presence of diagenetic xenotime. Xenotime is a common, trace phase in sedimentary rocks where it typically forms syntaxial overgrowths on detrital zircon grains (Rasmussen, 1996). With its high U content and low initial Pb concentration, it is ideal for U–Pb geochronology. Using an ion microprobe it is possible to date overgrowths as small as 10 μm, yielding highly precise U–Pb ages for diagenesis (McNaughton et al., 1999; Fletcher et al., 2000).

The sandstones collected in this study are moderately to well sorted, and texturally and compositionally mature. The samples range from mildly deformed and metamorphosed sandstone with intact syntaxial quartz overgrowths, to quartzites with recrystallized polygonal quartz, intergrown with coarse chlorite and muscovite crystals. Each sandstone examined contains detrital zircon (approximately 4000 grains in 56 PTS) of which 30% have outgrowths of xenotime (Fig. 2); however, less than 2% of outgrowths exceed 10 μm, the minimum size required for ion microprobe analysis. Examination by BSEM reveals the presence of distinct pyramidal overgrowths, as well as fine-scale, compositional zoning (Fig. 2a and b). Xenotime overgrowths are devoid of metamorphic matrix inclusions, and where metamorphic monazite abuts zircon, xenotime pyramids are partly surrounded by the monazite.

3. SHRIMP analytical procedures

Following petrographic examination by optical microscope and SEM, samples containing abundant, large xenotime overgrowths were selected for heavy liquid and magnetic separation. However, overgrowths greater than 5 μm in size did not survive the mineral separation process, and consequently, xenotime overgrowths larger than 10 μm were cut out of polished thin-sections and mounted in epoxy discs. Xenotime overgrowths and detrital grains were analyzed by SHRIMP following established procedures that include corrections for contributions to the secondary ion signal from adjacent zircon (Fletcher et al., 2000). Where zircon grains were too small for analysis, corrections were made assuming that the zircon was 2700 million years old, and contained 400 ppm of uranium. This will, on average, over-correct the xenotime data to produce young dates, and therefore, the minimum age determined from grouped data is considered to be conservative. The overall data pattern would be essentially the same if these data are omitted.

Corrections for common Pb were made by using the measured ^{204}Pb and the Pb isotopic composition of Broken Hill galena to remove the common Pb component from the measured isotopic ratios. Data used in age determinations are presented in Table 1, whereas data not used because of high proportions of zircon overlap ($Zr_2O^+/Y_2O^+ > 0.01$), high common Pb (>2% common Pb in ^{206}Pb) or textural ambiguity about the origin of the xenotime, are listed in Table 2. In both

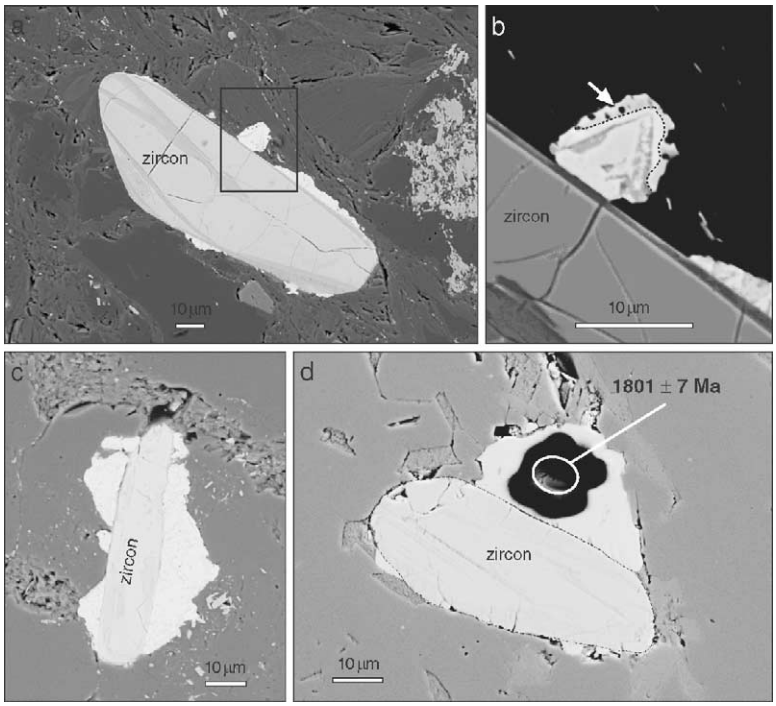

Fig. 2. Back-scattered scanning electron microscope (BSEM) images of detrital zircon grains with xenotime overgrowths. (a) Rounded zircon with several small xenotime overgrowths. (b) Closeup of xenotime overgrowth in A, showing a 'pyramidal' crystal surrounded by an irregular, compositionally different rim (arrow). Dotted line traces a compositional boundary within the rim. (c) Elongate zircon grain surrounded by broadly pyramidal diagenetic xenotime. (d) Rounded zircon with large xenotime overgrowth. The SHRIMP analytical spot (white outline) is surrounded by a region stripped of its gold coating (black). The spot correlates with analysis A85B.1-1a (Table 1) and the date refers to its corrected $^{207}Pb/^{206}Pb$ age (1σ precision).

tables, all isotopes are identified by mass number only, and uncertainties are 1σ and refer to the last digits given. The precision of Pb/Pb data is determined from counting statistics and scatter in the data profiles, and estimated uncertainties in the corrections for zircon overlap (Fletcher et al., 2000).

4. Diagenetic xenotime age data

Data for five detrital xenotime grains give concordant data (within precision) and $^{207}Pb/^{206}Pb$ dates >2100 Ma, consistent with data from detrital zircon and monazite (Table 1; Fig. 3). Thirty-two analyses of 20 xenotime overgrowths give $^{207}Pb/^{206}Pb$ dates between 1839 ± 16 Ma and 1458 ± 91 Ma (Table 1). The age distribution for the overgrowths has two prominent peaks (Fig. 3), possibly reflecting two main phases of growth. Mixture modeling (Sambridge and Compston, 1994) differentiates a distinct younger group at 1662 ± 15 Ma (95% confidence; $n = 13$ analyses; mean square of weighted deviates [MSWD] = 0.76), but the older peak is more complex. Nine analyses (from seven overgrowths) yielding the oldest dates, give a weighted mean $^{207}Pb/^{206}Pb$ age of 1800 ± 14 Ma (95% confidence; MSWD = 2.2), while four analyses of two overgrowths suggest an age of approximately 1825 Ma. Omitting data from this subset that rely on assumed zircon compositions gives an age of 1793 ± 10 Ma ($n = 6$; MSWD = 1.2). We interpret 1800 ± 14 Ma as a minimum age for sediment deposition. The significance of the younger xenotime age (i.e. 1662 ± 15 Ma) is uncertain, but probably relates to a thermal event that affected the basin.

Most of the U–Pb data for the xenotime overgrowths are discordant, but it is unclear whether this correctly records discordance in the samples. The xenotime overgrowths have unusually high concentrations

Table 1
SHRIMP U–Pb xenotime data

Grain-spot[a]	U (ppm)[b]	Th (ppm)[b]	Th/U	f206[c] (%)	$^{207}Pb/^{206}Pb$[d]	$^{206}Pb/^{238}U$[b]	Conc.[e] (%)	$^{207}Pb/^{206}Pb$ age (Ma)	Corrected $^{207}Pb/^{206}Pb$ age (Ma)[f]
Detrital grains									
B84B.2-1a	2084	2699	1.30	0.065	0.2265 ± 10	0.598	100	3028 ± 7	3028 ± 7
B84F.1-3a	7667	1351	0.18	1.063	0.1342 ± 4	0.399	100	2154 ± 5	2154 ± 5
B84F.1-2a	7293	694	0.10	0.011	0.1339 ± 3	0.405	102	2150 ± 4	2150 ± 4
A63C.2-1a	1034	1279	1.24	0.087	0.1302 ± 8	0.359	94	2100 ± 11	2100 ± 11
Diagenetic overgrowths									
A85F.2-1a	2789	40071	14.37	0.388	0.1130 ± 8	0.231	72	1848 ± 12	*1839 ± 16*
A85F.1-1a	2861	38847	13.58	0.352	0.1117 ± 6	0.241	76	1827 ± 10	*1822 ± 13*
B44.5-1a				1.087	0.1114 ± 15			1822 ± 25	1820 ± 26
A85F.1-1b				0.469	0.1113 ± 7			1821 ± 12	*1816 ± 15*
A85B.1-1a	2058	26489	12.87	0.034	0.1101 ± 4	0.298	93	1801 ± 7	1801 ± 7
A63′A1-1a	1620	26905	16.61	0.187	0.1097 ±6	0.279	88	1794 ± 10	1794 ± 10
B44.4-1b				0.902	0.1093 ± 13			1787 ± 22	1781 ± 25
A85B.1-1b				0.164	0.1087 ± 6			1778 ± 10	1778 ± 10
B45.6-1b				0.409	0.1085 ± 11			1775 ± 19	1774 ± 19
A63A.1-1b				0.089	0.1081 ± 8			1768 ± 14	1768 ±14
A63′A.1-1b				0.346	0.1083 ± 8			1772 ± 13	*1767 ± 16*
A63A.1-1a	1308	18186	13.91	0.215	0.1081 ± 6	0.293	94	1768 ± 10	1768 ± 10
A85C.1-1a	1959	26314	13.43	0.171	0.1081 ± 6	0.288	92	1767 ± 10	1767 ± 10
B44.9-1a				1.134	0.1073 ± 27			1753 ± 46	1753 ± 46
A85C.1-1b				0.186	0.1063 ± 6			1736 ± 10	1736 ± 10
B45.6-1a	2119	31350	14.80	0.569	0.1060 ± 10	0.284	93	1731 ± 18	1730 ± 18
B44.4-1a				1.828	0.1057 ± 25			1727 ± 43	1719 ± 47
B45.5-1a				0.691	0.1080 ± 23			1765 ± 38	1705 ± 68
B45.9-1b				0.351	0.1037 ± 13			1692 ± 23	1691 ± 23
B45.4-1a				0.983	0.1036 ± 17			1690 ± 30	1676 ± 37
A85A.1-1a	1167	15674	13.44	0.265	0.1028 ± 8	0.288	97	1675 ± 14	1675 ± 14
B45.3-1a	1933	26816	13.87	0.451	0.1023 ± 13	0.293	100	1666 ± 24	1665 ± 25
B45.3-1b				0.444	0.1021 ± 11			1664 ± 21	1663 ± 22
A63′C.1-1a	2752	55773	20.27	1.178	0.1027 ± 16	0.155	56	1674 ± 29	*1656 ± 38*
A63D.1-1a	1956	37944	19.40	1.768	0.1019 ± 16	0.220	77	1659 ± 29	*1654 ± 31*
A63C.1-1a	2677	54462	20.34	0.674	0.1028 ± 11	0.140	51	1675 ± 19	*1645 ± 34*
B45.9-1a	1687	19120	11.34	0.476	0.1011 ± 14	0.249	87	1644 ± 26	1644 ± 26
B45.2-1a				0.576	0.0999 ± 15			1623 ± 28	1619 ± 30
B44.11-1a				1.373	0.0991 ± 32			1607 ± 59	*1588 ± 68*
B44.3-1a				1.830	0.0988 ± 25			1602 ± 47	1581 ± 57
B45.2-1b				0.833	0.0969 ± 19			1565 ± 38	1562 ± 39
B44.6-1a				1.733	0.0930 ± 37			1489 ± 76	*1458 ± 91*

[a] Grain spot labels AnmX′.p-qa: Anm: mount number; X: fragment of polished thin section (blank for grain mounts); [′]: second analytical session; p: grain in thin section fragment or on grain mount; q: site on grain; a: measurement on site.
[b] U, Th and $^{206}Pb/^{238}U$ are not reported for second measurements or for cases where xenotime occupies <50% of primary beam area.
[c] 4f206 is the proportion of total ^{206}Pb determined to be common Pb.
[d] All Pb data are corrected for common Pb.
[e] Conc. is apparent concordance, defined as 100 × (t[$^{206}Pb/^{238}U$]/t[$^{207}Pb/^{206}Pb$]).
[f] Corrected for zircon overlap. Plain text entries required no correction or used measured zircon compositions. For entries in italics, zircon data are not obtainable and the correction assumes zircon contamination from a 2700 Ma zircon with 400 ppm U.

of Th, which might have affected Pb^+/U^+ ion production ratios in ways not covered by the U-only matrix correction. Also, many of the analytical spots overlapped the edges of the xenotime, and in most cases the primary beam was moved across the nearby sample surface for some time before analysis, in order to maximize xenotime coverage by the primary ion spot. Both of these factors can degrade Pb/U data. If

Table 2
SHRIMP U–Pb xenotime data not used in age determinations

Grain-sport[a]	U (ppm)[b]	Th (ppm)[b]	Th/U	4f206[c]	$^{207}Pb/^{206}Pb$[d]	$^{206}Pb/^{238}U$[d]	Conc.[e] (%)	$^{207}Pb/^{206}Pb$ age (Ma)	Correct $^{207}Pb/^{206}Pb$ age (Ma)[f]
Zr_2O^+/Y_2O^+ > 0.01 and zircon composition unknown									
B84H.1-1	2846	42144	14.81	0.468	0.1101 ± 6	0.297	93	1801 ± 10	*1779 ± 21*
B84H.1-2	2852	41034	14.39	0.658	0.1081 ± 7	0.285	92	1768 ± 12	*1742 ± 25*
A63′C.1-1b				1.695	0.1020 ± 19			1661 ± 34	*1604 ± 62*
High common Pb (4f206 > 2%)									
B45.8-1a	3145	48125	15.30	3.411	0.1097 ± 25	0.218	71	1794 ± 41	1764 ± 56
B44.7-1a				2.755	0.1072 ± 30			1753 ± 51	1752 ± 51
A63′D.1-1a	2061	56566	27.45	3.343	0.1024 ± 23	0.189	67	1668 ± 42	*1639 ± 57*
A85E.1-1a	179	1935	10.83	2.322	0.1022 ± 40	0.317	107	1664 ± 72	*1639 ± 85*
B45.10-1a				7.978	0.0971 ± 63			1569 ± 122	1566 ± 123
B45.1-1a				9.469	0.0921 ± 66			1470 ± 136	1468 ± 137
B44.1-1a				2.570	0.0846 ± 33			1306 ± 75	1291 ± 82
B45.1-1b				3.681	0.0836 ± 46			1283 ± 107	1282 ± 108
B44.2-1a				5.383	0.0824 ±86			1255 ± 206	923 ± 372
Texturally ambiguous xenotime grains[g]									
B84D.1-1a	10473	3210	0.31	0.021	0.1230 ± 3	0.370	101	2000 ± 4	2000 ± 4
B84D.1-2a	6119	5764	0.94	0.320	0.1050 ± 7	0.312	102	1715 ± 12	1715 ± 12
B84D.1-3a	5434	2622	0.48	0.111	0.1086 ± 6	0.311	98	1776 ± 10	1776 ± 10
B84F.1-1a	2333	15405	6.60	1.392	0.1218 ±13	0.361	100	1982 ± 19	1982 ± 19

[a] Grain spot labels AnmX′.p-qa: Anm: mount number; X: fragment of polished thin section (blank for grain mounts); [′]: second analytical session; p: grain in thin section fragment or on grain mount; q: site on grain; a: measurement on site.

[b] U, Th and $^{206}Pb/^{238}U$ are not reported for second measurements or for cases where xenotime occupies <50% of primary beam area.

[c] 4f206 is the proportion of total ^{206}Pb determined to be common Pb.

[d] All Pb data are corrected for common Pb.

[e] Conc. is apparent concordance, defined as $100 \times (t[^{206}Pb/^{238}U]/t[^{207}Pb/^{206}Pb])$.

[f] Corrected for zircon overlap. Plain text entries required no correction or used measured zircon compositions. For entries in italics, zircon data are not obtainable and the correction assumes zircon contamination from a 2700 Ma zircon with 400 ppm U.

[g] Data collected from xenotime whose origin is uncertain based on textures and compositional zoning. Grain B84D1 apparently preserves areas that are detrital in origin, retaining a pre-sedimentary age (1-1a), but also consists of areas that may be diagenetic (1-2a and 1-3a). Grain B84F has a distinct euhedral core (1-2a and 1-3a; Table 1) and a compositionally distinct overgrowth (1-1a) that is markedly older than other overgrowths; the entire grain could be detrital.

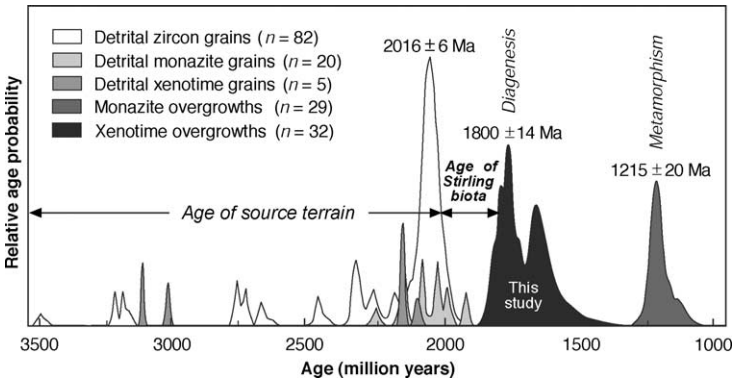

Fig. 3. Gaussian summation plot showing U–Pb age data for zircon, xenotime and monazite.

the samples really are discordant, this could be due to loss of radiogenic Pb, in which case the $^{207}Pb/^{206}Pb$ dates would have been reduced, so they still provide valid minimum ages. However, the preservation of concordant U–Pb systems in the detrital xenotime grains indicates that there has been no event causing pervasive Pb loss. We, therefore, consider that the overgrowths have not undergone Pb-loss and the apparent discordance is primarily due to limitations in data acquisition and Pb/U calibration. Since xenotime growth occurred over a prolonged period, some analyzed volumes will include zones of different age; data from these mixed zones would be genuinely discordant.

The xenotime overgrowths are unlikely to be detrital because of their irregular to euhedral shape (Fig. 2). A detrital origin is also inconsistent with the geochronological data, because the oldest xenotime overgrowths are 300 million years younger than the youngest unambiguous detrital xenotime grain (2100 ± 11 Ma), and 200 million years younger than the youngest zircon population (2016 ± 6 Ma) (Fig. 3). In addition, the xenotime overgrowths are chemically distinct, containing much higher Th concentrations (>1.5% Th; Th/U >12) than the analyzed detrital xenotime grains (<0.3% Th; Th/U <1.5).

A metamorphic origin for the xenotime overgrowths can also be discounted on the basis of petrographic and geochronologic evidence. Xenotime overgrowths are enclosed by metamorphic monazite cement, indicating that the xenotime formed earlier. Also, they are devoid of metamorphic mineral inclusions, in marked contrast to monazite overgrowths that contain hematite laths as well as metamorphic sericite and quartz (Rasmussen et al., 2002a). In addition, the oldest authigenic xenotime age population predates metamorphism, as dated by monazite (1215 ± 20 Ma) (Rasmussen et al., 2002a) and phyllosilicates (approximately 1190 Ma) (Harris, 1994), by 600 million years. Thus, early xenotime growth (approximately 1800 Ma) was almost certainly diagenetic, constraining sediment deposition to within a 200 million-year interval (Fig. 3), and possibly within 100 million years if data from a single detrital monazite grain (approximately 1895 Ma) are used to define the maximum age.

5. Discussion

Uranium–lead geochronology of xenotime overgrowths in the Stirling Range Formation indicates that the sediments were deposited before approximately 1800 Ma. Detrital zircon dates provide a maximum depositional age of approximately 2015 Ma (Rasmussen et al., 2002a), constraining the age of the succession to a 200 million-year interval. The data suggest that the Stirling Range Formation may be the same age or up to 300 million years older than the nearby Mount Barren Group (Fig. 1a), which is constrained between 1694 ± 4 Ma (Vallini et al., 2002) and approximately 1790 Ma (Dawson et al., 2002), based respectively, on diagenetic xenotime and detrital zircon age dating. Textural observations from the Mount Barren Group indicate that the xenotime overgrowths formed during early diagenesis, possibly near the sediment–water

interface, in which case the Stirling Range Formation must be at least 100 million years older. Nevertheless, the two successions may represent remnants of a once larger depositional basin, as proposed in earlier studies (Clarke et al., 1954; Sofoulis, 1958); further work is still required to establish the correlation.

Our results show that the various discoidal impressions and trace-like fossils in the Stirling Range Formation are more than 1800 million years old. If our interpretation of the trace-like fossils is correct, that is that they represent the casts of sediment-laden mucus strings formed by the movement of vermiform organisms (Rasmussen et al., 2002a; Bengtson et al., submitted), then motile multicellularity (or syncytiality) had already developed by the Paleoproterozoic. The trace–fossil interpretation of the documented structures has been challenged by Conway Morris (2002) and Budd and Jensen (2003), but their critical comments have failed to address the consistent and characteristic morphology of the presumed traces or to present a viable alternative interpretation (see Rasmussen et al., 2002b; Bengtson et al., submitted).

In combination with other evidence of probable multicellular life—the first alga-like, megascopic eukaryotes (Han and Runnegar, 1992; Hofmann, 1994; Zhu and Chen, 1995; Zhu et al., 2000; Porter and Knoll, 2000; Schneider et al., 2002)—the Stirling biota suggests that an evolutionary threshold was crossed some time in the Paleoproterozoic following a long period of environmental changes (Bengtson et al., submitted). The failure of large multicellular organisms to diversify until the latest Neoproterozoic may reflect environmental factors such as modest oxygen levels. While the evolutionary significance of the Paleoproterozoic megascopic biotas is still unknown, the commonly expressed view of an exclusively microbial biosphere during this time appears to need modification.

Acknowledgements

We thank the staff of the Centre for Microscopy and Microanalysis, University of Western Australia, for technical help, and the Department of Conservation and Land Management for permission to sample within the Stirling Range National Park. We thank Allen Nutman and Vladimir Sergeev for constructive reviews. B.R. acknowledges grants and a fellowship from the Australian Research Council (ARC). Zircon and xenotime analyses were performed on the Western Australian SHRIMP II operated by a WA university-government consortium with ARC support.

References

Beeson, J., 1991. A field and experimental study of structures in the Albany Mobile Belt, Western Australia. Ph.D. thesis, University of Western Australia, Crawley.

Bengtson, S., Rasmussen, B., Krapez, B., submitted. The Paleoproterozoic, megascopic Stirling biota. Paleobiology.

Black, L.P., Harris, L.B., Delor, C.P., 1992. Reworking of Archaean and early Proterozoic components during a progressive, middle Proterozoic tectonothermal event in the Albany Mobile Belt, Western Australia. Precambrian Res. 59, 95–123.

Boulter, C.A., 1979. On the production of two inclined cleavages during a single folding event Stirling Range, SW Australia. J. Struct. Geol. 1, 207–219.

Budd, G.E., Jensen, S., 2003. The limitations of the fossil record and the dating of the origin of the Bilateria. In: Donoghue, P.C.J. (Ed.), Telling the Evolutionary Time. Molecular Clocks and the Fossil Record. Taylor and Francis, London, pp. 166–189.

Clark, D.J., Hensen, B.J., Kinny, P.D., 2000. Geochronological constraints for a two-stage history of the Albany–Fraser Orogen, Western Australia. Precambrian Res. 102, 155–183.

Clark, D.J., Kinny, P.D., Post, N.J., Hensen, B.J., 1999. Relationships between magnetism, metamorphism and deformation in the Fraser Complex, Western Australia: constraints from new SHRIMP U–Pb zircon geochronology. Aust. J. Earth Sci. 46, 923–932.

Clarke, E.C., Phillips, H.T., Prider, R.T., 1954. The Precambrian geology of part of the south coast of Western Australia. J. R. Soc. West. Aust. 38, 1–64.

Conway Morris, S., 2002. Ancient animals or something else entirely? Science 298, 57–58.

Cruse, T., 1991. The sedimentology, depositional environment and Ediacaran fauna of the Stirling Range Formation, Western Australia. B.Sc. Hons. thesis, University of Western Australia, Crawley.

Cruse, T., Harris, L.B., 1994. Ediacaran fossils from the Stirling Range Formation, Western Australia. Precambrian Res. 67, 1–10.

Cruse, T., Harris, L.B., Rasmussen, B., 1993. The discovery of Ediacaran trace and body fossils in the Stirling Range Formation, Western Australia: implications for sedimentation and deformation during the 'Pan-African' orogenic cycle. Aust. J. Earth Sci. 40, 293–296.

Dawson, G.C., Krapez, B., Fletcher, I.R., McNaughton, N.J., Rasmussen, B., 2002. Did late Palaeoproterozoic assembly of proto-Australia involve collision between the Pilbara, Yilgarn and Gawler Cratons? Geochronological evidence from the Mount Barren Group in the Albany–Fraser Orogen of Western Autralia. Precambrian Res. 118, 195–220.

Dawson, G.C., Krapez, B., Fletcher, I.R., McNaughton, N.J., Rasmussen, B., 2003. 1.2 Ga thermal metamorphism in the Albany–Fraser Orogen of Western Australia: consequences of collision or regional heating by dyke swarms? J. Geol. Soc. Lond. 160, 29–37.

Fletcher, I.R., Rasmussen, B., McNaughton, N.J., 2000. SHRIMP U–Pb geochronology of authigenic xenotime and its potential for dating sedimentary basins. Aust. J. Earth Sci. 47, 845–860.

Han, T.-M., Runnegar, B., 1992. Megascopic eukaryotic algae from the 2.1 billion-year-old Negaunee Iron-Formation, Michigan. Science 257, 232–235.

Harris, L.B., 1994. Neoproterozoic sinistral displacement along the Darling Mobile Belt, Western Australia, during Gondwanaland assembly. J. Geol. Soc. Lond. 151, 901–904.

Harris, L.B., Beeson, J., 1993. Gondwanaland significance of Lower Palaeozoic deformation in central India and SW Western Australia. J. Geol. Soc. Lond. 150, 811–814.

Harris, L.B., Li, Z.-X., 1995. Palaeomagnetic dating and tectonic significance of dolerite intrusions in the Albany Mobile Belt, Western Australia. Earth Planet. Sci. Lett. 131, 143–164.

Hofmann, H.J., 1994. Proterozoic carbonaceous compression ("metaphytes" and "worms"). In: Bengtson, S. (Ed.), Early Life on Earth. Columbia University Press, New York, pp. 342–357.

McNaughton, N.J., Rasmussen, B., Fletcher, I.R., 1999. SHRIMP uranium–lead dating of diagenetic xenotime in siliciclastic sedimentary rocks. Science 285, 78–80.

Muhling, P.C., Brakel, A.T., 1985. Mount Barker-Albany 1:250 000 Geological Series—Explanatory Notes. Geological Survey of Western Australia, Perth.

Porter, S., Knoll, A.H., 2000. Testate amoebae in the Neoproterozoic Era: evidence from vase-shaped microfossils in the Chuar Group, Grand Canyon. Paleobiology 26, 360–385.

Rasmussen, B., 1996. Early-diagenetic REE-phosphate minerals (florencite, gorceixite, crandallite and xenotime) in marine sandstones: a major sink for oceanic phosphorus. Am. J. Sci. 296, 601–632.

Rasmussen, B., Fletcher, I.R. (in press). Zirconolite: a new UP-b chronometer for mafic igneous rocks. Geology.

Rasmussen, B., Bengtson, S., Fletcher, I.R., McNaughton, N.J., 2002a. Discoidal impressions and trace-like fossils more than 1200 million years old. Science 296, 1112–1115.

Rasmussen, B., Bengtson, S., Fletcher, I.R., McNaughton, N., 2002b. Ancient animals or something else entirely? Science 298, 58–59.

Sambridge, M.S., Compston, W., 1994. Mixture modelling of multi-component data sets with application to ion-probe zircon ages. Earth Planet. Sci. Lett. 128, 373–390.

Schneider, D.A., Bickford, M.E., Cannon, W.F., Schulz, K.J., Hamilton, M.A., 2002. Age of volcanic rocks and syndepositional iron formations, Marquette Range Supergroup: implications for the tectonic setting of Paleoproterozoic iron formations of the Lake Superior region. Can. J. Earth Sci. 39, 999–1012.

Sofoulis, J., 1958. Notes on the reconnaissance of the Stirling Range area, south–west division. West. Aust. Geol. Surv. Bull. 109, 68–80.

Turek, A., Stephenson, N.C.N., 1966. The radiometric age of the Albany Granite and the Stirling Range Beds, southwest Australia. J. Geol. Soc. Aust. 13, 449–456.

Vallini, D., Rasmussen, B., Krapez, B., Fletcher, I.R., McNaughton, N.J., 2002. Obtaining diagenetic ages from metamorphosed sedimentary rocks: U–Pb dating of unusually coarse xenotime cement in a phosphatic sandstone. Geology 30, 1083–1086.

Zhu, S., Chen, H., 1995. Megascopic multicellular organisms from the 1700-million-year-old Tuanshanzi Formation in the Jixian area North China. Science 270, 620–622.

Zhu, S., Sun, S., Huang, X., He, Y., Zhu, G., Sun, L., Zhang, K., 2000. Discovery of carbonaceous compressions and their multicellular tissues from the Changzhougou Formation (1800 Ma) in the Yanshan Range, North China. Chin. Sci. Bull. 45, 841–847.